J Biomol NMR (2009) 45:311–318
DOI 10.1007/s10858-009-9372-5

ARTICLE

Time-shared HSQC-NOESY for accurate distance constraints measured at high-field in ^{15}N-^{13}C-ILV methyl labeled proteins

Dominique P. Frueh · Alison Leed · Haribabu Arthanari · Alexander Koglin · Christopher T. Walsh · Gerhard Wagner

Received: 26 June 2009 / Accepted: 20 August 2009 / Published online: 2 September 2009

Abstract We present a time-shared 3D HSQC-NOESY experiment that enables one to simultaneously record ^{13}C- and ^{15}N-dispersed spectra in Ile, Leu and Val (ILV) methyl-labeled samples. This experiment is designed to delineate the two spectra which would otherwise overlap with one another when acquired together. These spectra display nOe correlations in the detected proton dimension, i.e. with maximum resolution. This is in contrast to NOESY-HSQC types of experiments that provide cross-peaks in the indirect dimension with low resolution due to limits in experimental time. The technique is particularly advantageous at high field where even longer experimental times would be required for comparable resolution in NOESY-HSQC experiments. The method is demonstrated at 900 MHz and at 750 MHz on 37 and 31 kDa proteins, respectively. The resolution and time saving provided in this experiment was crucial for solving the structures of these two proteins.

Keywords Protein structure · Distance constraints · Nuclear magnetic resonance · Non-ribosomal peptide synthetases · Time-shared · High-resolution · NOESY

D. P. Frueh · A. Leed · H. Arthanari · A. Koglin · C. T. Walsh · G. Wagner (✉)
Department of Biological Chemistry and Molecular Pharmacology, Harvard Medical School, 240 Longwood Avenue, Boston, MA 02115, USA
e-mail: Gerhard_Wagner@hms.harvard.edu

Present Address:
A. Koglin
Bioenergy, Environmental Science Bioscience Division B-8, Los Alamos National Laboratory, Bikini Atoll Drive, Los Alamos, NM 87545, USA

Introduction

Nuclear magnetic resonance is routinely used nowadays to determine structures of biomolecules. Key to this success is the ability to determine distance constraints from nuclear Overhauser effects measured in NOESY experiments. In large proteins, or more generally, for molecules with crowded NMR spectra, selective labelling of specific nuclei is routinely performed to simplify the spectra and minimize relaxation losses. The most popular strategy relies on using a sample which is selectively protonated and ^{13}C-enriched at the methyls of Leu, Val and Ile (at the δ1 position) in an otherwise deuterated, ^{12}C background. The molecule is typically uniformly enriched in ^{15}N so that, when in H_2O, nOes involving amide protons or methyl protons can be measured with the same sample. This sparse labelling approach eliminates many ambiguities in nOe cross-peak assignments but obviously reduces the number of observable nOes drastically. Therefore it becomes critical to resolve and unambiguously assign a maximum number of the observed NOE cross-peaks. This can be achieved by recording several multidimensional experiments which disperse the nOe cross-peaks of 2D spectra along a third dimension, provided by correlated ^{13}C or ^{15}N nuclei in 3D experiments. Further dispersion of nOe cross-peaks can be achieved by including an additional, fourth heteronuclear dimension in 4D experiments. This increase in the number of experiments is accompanied by an increase in precious spectrometer acquisition time. We recently showed how the two ^{15}N- and ^{13}C-edited 3D spectra can be recorded in a single TS-NOESY-PEP-HSQC/TROSY experiment, while a second experiment allows for the four possible 4D spectra to be acquired simultaneously (Frueh et al. 2006). This was achieved by implementing time-shared transfers and evolutions (Sørensen 1990; Farmer 1991; Boelens

et al. 1994; Pascal et al. 1994; Jerala and Rule 1995; Sattler et al. 1995), a method which has recently found many new applications in biomolecular NMR (Uhrín et al. 2000; Xia and Zhu 2001; Kupce et al. 2003; Frueh et al. 2005, 2006; Perez-Trujillo et al. 2007; Wurtz et al. 2007; Guo and Tugarinov 2009). While the 4D experiment leads to unambiguous assignment of nOe cross-peaks and the 3D experiment enables their integration, the latter suffers from limited resolution in the dimension displaying the nOe correlations and part of the improvement obtained from the technique is deteriorated during peak integration due to signal overlap. This limitation results from using NOESY-HSQC based experiments, where the nOe cross-peaks appear in an indirect dimension, which can only achieve a relatively low resolution for typical acquisition times. To overcome this shortcoming, we developed a variant of the 3D time-shared experiment based on the HSQC-NOESY experiment which provides the desired dipolar correlations in the detected dimension to maximize the resolution of nOe cross-peaks. The higher resolution achieved makes up for any reduced sensitivity from the inability to use TROSY efficiently (and an increased length of the pulse sequence for a water suppression scheme) because more accurate volume integrations become possible. Because nOe cross-peaks appear in the detected dimension, the cross-peaks of one pathway (e.g. ^{15}N-dispersed) overlap with those of the other pathway (e.g. ^{13}C-dispersed), as well as with the strong diagonal peaks. The TS-HSQC-NOESY experiment has thus been designed to delineate the ^{15}N- and ^{13}C-edited spectra that would otherwise overlap. The method is demonstrated on the 37 kDa T-TE di-domain of the enterobactin EntF non-ribosomal peptide synthetase (NRPS) and the 31 kDa regulatory subunit of γ-glutamyl-cysteine synthetase (γGCS). The high resolution provided by this experiment was absolutely crucial for solving these structures (Frueh et al. 2008; Leed et al. in preparation).

Materials and methods

For both proteins, an expression plasmid (pET30a+ for the point mutant S48A-TTE and pBluescript SK- for γGCS) containing the full length cDNA for the N-terminally His_6-tagged protein was transformed into *E. coli* BL21(DE3) cells. A ^{15}N ^{2}H uniformly labeled sample, with protonated Phe and Tyr residues and with selective protonation and ^{13}C labelling of the methyl carbons of Ile (δ position only), Leu and Val side-chains, was prepared by over-expression in M9 minimal medium in D_2O containing ^{2}H glucose and $^{15}NH_4Cl$. Protons also occur at the β position of Val and at the γ positions of Ile and Leu (except for the γGCS sample used to record the TS-HSQC-NOESY). The cells were initially allowed to grow at 37°C until 1 h before induction (O.D. $\sim$ 0.4). At this point, 2-oxo-3-(^{13}C-methyl)-4-^{13}C-butanoate ($^{13}C_2$-dimethyl-α-ketoisovalerate), 2-oxo-4-^{13}C-butanoate (^{13}C-methyl-α-ketobutyrate), ^{15}N-phenylalanine and ^{15}N-tyrosine were added to the growth medium. When the optical density reached $\sim$0.6, the bacteria were induced with 1 mM IPTG and the medium was cooled to 25°C and allowed to grow overnight. Recombinant protein samples were purified using Ni-NTA resin (Qiagen) followed by FPLC using a Sephadex gel-filtration column (S75 for S48A-TTE and S200 for γGCS). The S48A-TTE sample was concentrated to a final concentration of 300 μM in 20 mM phosphate (pH 6.7), 150 mM NaCl, 1 mM EDTA and 1 mM DTT in 95% H_2O 5% D_2O. γGCS was concentrated to 500 μM (sample used for the time-shared NOESY-HSQC/TROSY) or 300 μM (sample used for the time-shared HSQC-NOESY). The γGCS NMR buffer contained 50 mM Tris-*d11* (pH 7.25), 100 mM NaCl, 5 mM $MgCl_2$, and 10 mM DTT-*d10*. The γGCS sample used for the TS-HSQC-NOESY was prepared with α-keto-acid precursors deuterated at the alpha position of the ketone.

The S48A-TTE data were recorded at 25°C on a 900 MHz Bruker spectrometer equipped with a cryoprobe®. A mixing time of 200 ms was used in order to detect long-range nOes. The spectral widths were 16.023 ppm for proton (ω_3, centred at 4.690 ppm), 35 ppm for nitrogen (ω'_1, centred at 118 ppm), 22 ppm for carbon (ω_1, centred at 17 ppm) and 5 ppm for the indirect proton dimension (ω_2, centred at 8.5 ppm). A data matrix of 1,024 × 78 × 120 complex points was acquired for these nuclei, respectively. A recycling delay of 1 s was used, and for each value of t_1, t'_1, t_2, t'_2, two FIDs, each with 8 scans accumulated, were recorded in an interleaved manner with a different phase combination (see below). The total measurement time was 4 days and 17 h. The spectrum was linearly predicted and zero-filled to a final size of 2,048 (ω_3) × 156 (ω_1/ ω'_1) × 240 (ω_2) points.

The γGCS spectra for both the TS-NOESY-PEP-HSQC/TROSY and TS-HSQC-NOESY were recorded on a 750 MHz Bruker spectrometer equipped with a cryoprobe®. For each measurement, 1,024 (ω_3, ^{1}H) × 50 (ω_2, ^{13}C and ^{15}N) × 152 (ω_1, ^{1}H indirect) complex points were acquired. The TS-NOESY-PEP-HSQC/TROSY was acquired with 16 scans and the TS-HSQC-NOESY was acquired with 2 × 8 scans recorded in an interleaved fashion for two different value of the phase ϕ_2. Each experiment lasted 5 days and 15 h. The spectral widths were 16.023 ppm for proton (ω_3, centred at 4.690 ppm), 35 ppm for nitrogen (ω'_1, centred at 119.5 ppm) and 20 ppm for carbon (ω_1, centred at 18.5 ppm). For the TS-HSQC-NOESY, 5 ppm was used for the indirect proton dimension (ω_2, centred at 8.5 ppm), while 13 ppm was used for the TS-NOESY-PEP-HSQC/TROSY. The mixing time was 200 ms in both experiments.

For the two TS-HSQC-NOESY measurements, the two sub-matrices obtained with different phases were extracted from the raw data. The sum of the matrices led to spectra featuring nOes involving amide protons, while their difference led to spectra containing nOes involving methyl protons. The amide and methyl regions of the detected dimension were separated, and the resulting spectra were referenced according to the appropriate heteronuclei. All spectra were processed with the nmrPipe suite (Delaglio et al. 1995) and analysed with CARA (Keller 2004). All dimensions were zero-filled once and indirect dimensions were linearly predicted.

Results and discussion

Pulse sequence

The experiment presented here follows the principle of the time-shared technique (Sørensen 1990; Farmer 1991) used to simultaneously obtain ^{13}C-HSQC-NOESY and ^{15}N-HSQC-NOESY spectra.

In short, concatenated INEPT modules allow simultaneous transfers of polarization from amide and methyl protons to nitrogens and carbons, respectively (Fig. 1). A joint evolution of ^{13}C and ^{15}N single-quantum coherences (SQC) is tailored to provide optimal resolution in each dimension and minimize relaxation losses (see toggling frame in Fig. 1) (Boelens et al. 1994). Nitrogen SQC evolves during $t'_1 + t_1$, with time increments $\Delta t'_1 = 1/\mathrm{SW(N)} - 1/\mathrm{SW(C)}$ and $\Delta t_1 = 1/\mathrm{SW(C)}$, while carbon SQC only evolves during t_1 with the increment $\Delta t_1 = 1/\mathrm{SW(C)}$. A time-shared reverse INEPT is followed by a proton evolution period that encodes for the signals of the source protons. A mixing time is followed by a WATERGATE (Piotto et al. 1992) scheme. The water suppression can be done in this manner since amide and methyl protons resonances are very distinct from the water resonance. The magnetization flow can be summarized by:

$$\begin{cases} \mathrm{H^N} \xrightarrow{\mathrm{J(NH)}} \mathrm{N}(t_1 + t'_1)(a-d) \xrightarrow{\mathrm{J(NH)}} \mathrm{H^N}(t_2)(e) \xrightarrow{\mathrm{NOE}} \mathrm{H(f)} \\ \mathrm{H^{Me}} \xrightarrow{\mathrm{J(CH)}} \varphi_2\mathrm{C}(t_1)(b-c) \xrightarrow{\mathrm{J(CH)}} \varphi_2\mathrm{H^{Me}}(t_2)(e) \xrightarrow{\mathrm{NOE}} \varphi_2\mathrm{H(f)} \end{cases} \quad (1)$$

where $\varphi_2 = +1$ or -1, depending on the value of ϕ_2, and where H denotes all protons dipolar-coupled to the selected amide or methyl protons. For the samples in this study, these protons are the amide H^N, the δ-Ile, δ-Leu and γ-Val methyl H^{Me}, the Val H^{β}, the Ile and Leu H^{γ}, all Phe and all Tyr protons. Thus, two 3D spectra featuring either the nOe correlations $H^{Me} \rightarrow H$ or $H^N \rightarrow H$ are obtained simultaneously, where the arrow indicates the transfer of magnetization occurring during the mixing time. The nOe signals appear along the detected dimension and thus benefit from maximum resolution at no cost in experimental time. However, the cross-peaks of one pathway overlap with those of the other pathway in the detected dimension, so that the experiment cannot be used as such (Figure 2a and b). Signals that are dispersed in ^{13}C, i.e. from the $H^{Me} \rightarrow H$ pathway, appear in the same region as those that are ^{15}N-edited. This impedes the assignment of nOe signals and renders the experiment impractical. To enable delineation of the two spectra, interleaved experiments are recorded in which the phase ϕ_2, which selectively affects one pathway, is alternated. Addition and subtraction of the two datasets then provide the individual spectra of the ^{13}C-HSQC-NOESY and ^{15}N-HSQC-NOESY experiments (see below).

For larger proteins and/or for higher resolutions in the indirect dimensions, TROSY versions of the $H^N \rightarrow H$ pathway may need to be used. Our previous NOESY-HSQC type experiment was indeed designed to allow for the exploitation of TROSY. Improved versions of the H-N/C time-shared HN-TROSY/HC-HSQC building block, as designed by Permi and co-workers (Wurtz et al. 2007) or Tugarinov et al. (Guo and Tugarinov 2009), may be used in lieu of the HSQC block (between a and e in Fig. 1). However, these need to be modified to allow for sensitivity improvement when ^{15}N encoding takes place before the mixing time (i.e. in order to preserve N- and P- pathways) as previously developed (Brutscher et al. 1998; Meissner and Sorensen 1999; Zhu et al. 1999). The experiment then benefits from further sensitivity enhancement in the $H^N \rightarrow H$ pathway, when compared to NOESY-TROSY, since the native ^{15}N polarization contributes to the detected signal. When designing the time-shared experiment, care must be taken in order to maintain optimized transfers for both pathways, in particular when recording the four FIDs that are necessary for sensitivity enhanced TROSY $H^N \rightarrow N$ pathway. One drawback is that the water suppression can not be concatenated with the polarization transfers, unlike in NOESY-HSQC derived experiments. This, together with the use of proton shaped-pulses to independently manipulate amide and methyl protons, may deteriorate the advantages of the experiment. Such an experiment may prove useful, however, when used in conjunction with non-uniform sampling (NUS) (Barna et al. 1987; Schmieder et al. 1993; Orekhov et al. 2001), where long values of the evolution times t_1 and t_2 can be recorded, providing optimal resolution in all dimensions. Recent studies, carried out in parallel to the work presented here, indicate that NUS may be applied reliably to NOESY experiments of large proteins (Hyberts et al. 2009).

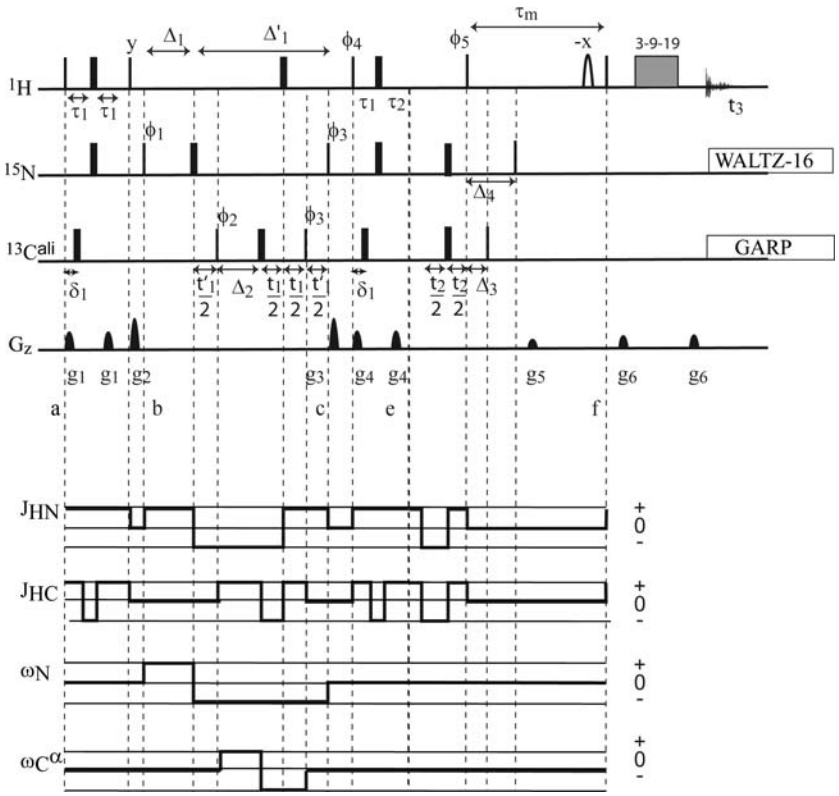

Fig. 1 Pulse sequence of the 3D TS-HSQC-NOESY experiment. *Narrow* and *wide solid rectangles* indicate 90° and 180° pulses, respectively. The pulses are applied along the x axis unless otherwise specified. A 800 μs 90° Sinc1 pulse (2,000 Hz bandwidth) is used to selectively excite the water (at 4.69 ppm). The delays are: $\tau_1 = 2.77$ ms $\approx 1/(4\ \mathrm{J(NH)})$, $\tau_2 = \tau_1 - t_2(0) -$ larger(τ_{180}(N),τ_{180}(C)), $\delta_1 = 1.786$ ms $\approx 1/(4\ \mathrm{J(CH)})$, $\Delta_1 = t'_1(0) + t_1(0) + \Delta_2 + 2\tau_{90}(\mathrm{C}) + \tau_{180}(\mathrm{H}) + \tau_{180}(\mathrm{C}) = 126$ μs, $\Delta_2 = t_1(0) + \tau_{180}(\mathrm{H}) = 29$ μs. $\Delta_3 = 3.572$ ms $\approx 1/(2\ \mathrm{J(CH)})$, $\Delta_4 = 5.554$ ms $\approx 1/(2\ \mathrm{J(NH)})$. The short delay Δ'_1 refocuses evolution under ^{15}N chemical shifts during the spin manipulation that occurs in Δ'_1. In the absence of ^{15}N and ^{13}C SQC encoding, for $t_1(0)$ and $t'_1(0)$, then $\Delta_1 = \Delta'_1$. Quadrature detection is achieved by the States-TPPI technique (Marion et al. 1989) applied to the phases ϕ_1 and ϕ_2 for t_1 evolution and on phase ϕ_4 for t_2 evolution. The time increments are set to $\Delta t_1 = 1/\mathrm{SW(C)}$ and $\Delta t'_1 = 1/\mathrm{SW(N)} - 1/\mathrm{SW(C)}$. The block labelled 3-9-19 is a WATERGATE (Piotto et al. 1992) water suppression scheme. Carbon decoupling is achieved by using a GARP (Shaka et al. 1985) sequence with field strength of 3.57 kHz. Nitrogen decoupling is achieved by using a WALTZ-16 sequence (Shaka et al. 1983) with field strength of 1.5 kHz. The phase cycle is $\phi_1 = x, -x$, $\phi_2 = -x, x$, $\phi_3 = 4(x), 4(-x)$, $\phi_4 = 8(x), 8(-x)$ with $\phi_{\mathrm{rec}} = x, -x, -x, x, -x, x, x, -x$. Pulses are applied on resonance with water during the sequence except for the pulse with phase ϕ_4, which is applied at 8.5 ppm. The phase ϕ_5 is shifted by 45° to allow for radiation damping to restore the water magnetization to $+z$ at the end of the mixing time (Talluri and Wagner 1996). At low fields and/or for short mixing times and/or in the absence of cryoprobes, water flip-back pulses (Grzesiek and Bax 1993) can easily be implemented. It is then best to replace the proton inversion pulse in Δ'_1 with a selective pulse inverting only amide protons. Sine-shaped gradients are applied with lengths and powers of: $g_1 = g_3 = (1$ ms, 6.5 G/cm), $g_2 = (1$ ms, 21.5 G/cm), $g_4 = (500$ μs, -9 G/cm), $g_5 = (1$ ms, 8.5 G/cm) and $g_6 = (1$ ms, 27 G/cm). All gradients are followed by a recovery delay of 200 μs. Every other FID is recorded with the phase ϕ_2 inverted (see text). *Bottom* Toggling frame (Chiarparin et al. 1999) diagram depicting evolutions under various interactions. Between points b and c, evolution under J(NH) occurs during $t'_1(0) + t_1(0) + 2\tau_{90}(\mathrm{C}) + \tau_{180}(\mathrm{H}) =$ c.a. 67 μs, and evolution under J(CH) occurs during $\Delta_2 = 29$ μs. While the first evolution can be cancelled by application of a 180° proton pulse during Δ_1, this results in deterioration of the water suppression

Data analysis and application to structure determination

The method described above is illustrated below for two different systems: a 37 kDa segment of a non-ribosomal peptide synthetase and a 31 kDa regulatory subunit of an enzyme involved in the synthesis of glutathione.

The amide and methyl spectra first need to be extracted from the data matrix by recombining the two sub-spectra. Figure 2a, b show the H/CN projections of the 3D spectra recorded in an interleaved manner. The sum of these spectra leads to the ^{15}N-dispersed HSQC-NOESY spectrum (Fig. 2c), while their difference results in the ^{13}C-dispersed spectrum (Fig. 2d). Each dataset is then independently referenced according to the appropriate nuclei and the indirect methyl proton dimension is circular shifted to compensate for spectral aliasing. The H/H$^{\mathrm{N}}$ and H/H$^{\mathrm{C}}$ projections are shown in Fig. 2e and f, respectively. The resulting ^{13}C- and ^{15}N-dispersed spectra are indistinguishable from those obtained with the individual experiments.

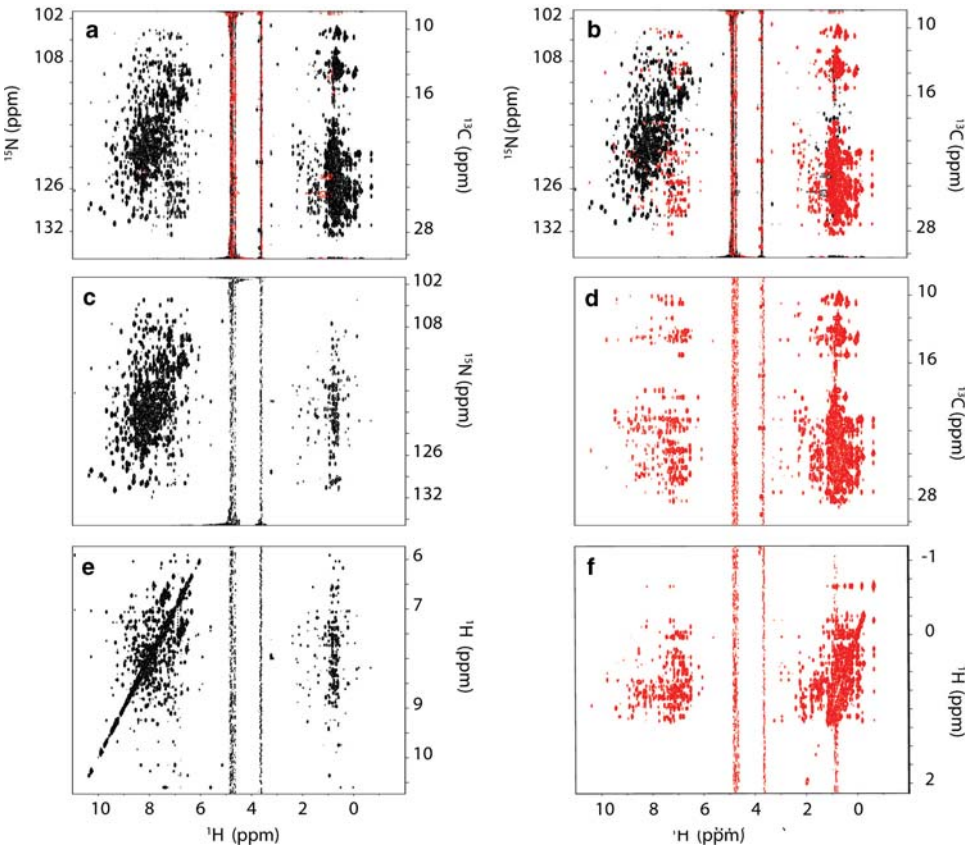

Fig. 2 Processing of the 3D TS-HSQC-NOESY experiment recorded on the 37 kDa S48A-TTE. **a** H/NC mixed projection of the 3D experiment. **b** The signals correlated to carbons are inverted by a 180° phase shift of ϕ_2 ($\varphi_2 = -1$ in Eq. 1). **c** The sum of a and b provides the ^{15}N-dispersed spectrum, while their difference **d** provides the ^{13}C-dispersed spectrum. **e** H/H^{N} projection. **f** H/H^{C} projection: the spectrum is circular shifted in ω_2 to centre the aliphatic protons

The motivation to develop this method stemmed from difficulties in solving the structure of the 37 kDa T-TE di-domain of the EntF component of the *E. coli* enterobactin synthetase (Frueh et al. 2008). Initially, distance constraints were identified on a sample of the apo-form of this protein by using the time-shared 3D and 4D experiment described in (Frueh et al. 2006). Indeed one of two proton dimensions of the 4D spectra is in the detected dimension and thus benefits from the ultra-high resolution as in the experiment proposed here. However, the 4D experiment has significantly lower sensitivity than the 3D experiment. Moreover, the three indirect dimensions are constrained to much lower resolutions than in the 3D spectra to maintain a reasonable acquisition time. Thus, while the 4D is immensely beneficial for cross-peak assignment, it is in general not suitable for volume integration which is hence performed in the 3D spectra. Unfortunately, when going to the time-shared 3D NOESY as described in (Frueh et al. 2006) it became apparent that the resolutions along the nOe dimensions were too poor to allow for automated signal integration of many of the constraints that were determined in the 4D spectra. We thus developed the technique presented here to provide maximal resolution in the NOESY dimension, with a reasonable experimental time. This was further motivated by the desire to exploit the advantages of a recently acquired 900 MHz spectrometer. Indeed, for an identical number of points in a given dimension, and thus for the same experimental time, the resolution is actually lower at higher fields due to shorter dwell times. Thus, longer experimental times are needed at high fields to overcome the reduction in dwell time. 2,048 complex points are traditionally collected in the detected dimension. When the nOes are in this dimension, this crowded spectrum benefits from a digital resolution of 7 Hz for a spectral width of 16 ppm. To achieve such resolution in an indirect dimension, as in NOESY-HSQC derived experiments, would take 34 min per FID. With 8 transients accumulated, this translates to roughly 5 h per plane for a total time of approximately 21 days, assuming 50 complex points in the heteronuclear dimension. In the time-shared NOESY-HSQC the indirect dimension can be reduced to 5 ppm since it only contains either amide protons (^{15}N-dipersed) or methyl protons (^{13}C-dispersed) so that the maximum time would be 6 days and 7 h. In addition, a much lower resolution is needed in the proton indirect dimension of HSQC-NOESY experiments. Indeed, this dimension here only contains one signal per residue (amide and Ile methyl) or two signals per residue (Val, Leu methyls). Thus the experimental time can be further reduced to about two days. Note that here we only consider cases where sensitivity is not an issue, and our comparison focuses solely on resolution. We did not account for

sensitivity improvements that can be achieved with TS-NOESY-HSQC derived experiments (TROSY, PEP, Methyl-TROSY) (Frueh et al. 2006; Wurtz et al. 2007; Guo and Tugarinov 2009).

The time-shared HSQC-NOESY experiment was recorded at 900 MHz on an S48A mutant of the T-TE di-domain. This mutation improves sample homogeneity and limits conformational exchanges in the T-domain (Koglin et al. 2006). The ^{13}C-HSQC-NOESY and ^{15}N-HSQC-NOESY spectra of this protein were used to illustrate Fig. 2. Using only amide to amide and amide to methyl nOes ($H^N \rightarrow H^N$ and $H^N \rightarrow H^{Me}$), the average rmsd of a structural bundle obtained by integrating these spectra is 5.7 Å (calculated by aligning α carbons in secondary structure elements of 10 structures). This relatively large value results from slowly exchanging amide protons that account for about 30% of the TE domain and which are absent from the calculation. For comparison, the structure of the apo sample, obtained with the 3D TS-NOESY-PEP-HSQC/TROSY had a larger rmsd of 9.2 Å. The improvement obtained with the TS-HSQC-NOESY data is the result of many parameters: (1) many new nOes could be observed as a result of the increase in resolution (nOes which could not be observed in the less sensitive 4D experiment), (2) the majority of the signals could be integrated and did not require arbitrary interpretation of signal overlap, and (3) NOESY cross-peak assignments could be corrected: several ambiguous constraints were erroneously attributed to short-range interactions in the NOESY-HSQC spectra when in fact they consisted of both long-range and short-range nOes or in some cases only long range constraints. These constraints could be unambiguously reassigned in the HSQC-NOESY version which allowed differentiation between two candidates. Thus, 259 long range nOes were observed in the NOESY-HSQC derived spectra, whereas the HSQC-NOESY allowed the identification of 272 long range constraints. The fold obtained with the HSQC-NOESY pair of spectra was then used as a basis to identify more nOes involving aliphatic protons in an ^{15}N-dispersed NOESY-TROSY, recorded on a uniformly protonated sample of S48A-TTE. In the end, we obtained a structural bundle with an rmsd of 1.2 Å (Frueh et al. 2008) (including all data, as well as hydrogen bond and torsion angle constraints). The method presented here was decisive in elucidating the structure of this 37 kDa protein.

To compare the TS-NOESY-HSQC/TROSY and TS-HSQC-NOESY, both experiments were recorded for the 31 kDa regulatory subunit of γ-glutamyl-cysteine synthetase (γGCS). In both experiments, the same number of complex points in the ^{13}C, ^{15}N and ^{1}H dimensions were collected; thus, the total measuring times were identical. However, slow aggregation prevented the use of the same sample for both experiments and thus, the sensitivity cannot be compared in these two spectra. The relatively short lifetime of the samples was another motivation to use the time-shared strategy and obtain ^{15}N- and ^{13}C-dispersed spectra at once. A quick assessment of the relative sensitivity was performed for a 38 kDa protein by recording H/NC 2D planes of the TS-HSQC-NOESY and the TS-NOESY-HN-TROSY/HC-HSQC experiment as improved by (Wurtz et al. 2007). For 39 complex points in the ^{15}N, ^{13}C mixed dimension, the TROSY version provided about 30% more signal. In the discussion that follows, only resolution is considered.

Figure 3 shows representative strips obtained for γGCS with these two experiments. A simple inspection reveals the advantages of the HSQC-NOESY experiment at high-field. Figure 3a displays amide to amide strips obtained with the NOESY-TROSY spectrum. Only sequential nOe cross-peaks can be observed between residues 202 and 203. The higher resolution of the HSQC-NOESY experiment (Fig. 3b) reveals additional long range cross-peaks (with 226 and 228 for 202 and with 180 and 181 for 203) that were obfuscated in the NOESY-TROSY spectrum. The situation is even more dramatic in the methyl to methyl region of the ^{13}C-dispersed spectrum. Most cross-peaks overlap in the NOESY-PEP-HSQC spectrum, and only a few signals can be assigned (e.g. 166 δ1 and 175 δ1 to 166 δ2). The HSQC-NOESY spectrum provides five more constraints. In addition the overlap is so severe in the NOESY-HSQC that peak integration would be unreliable for structure calculations.

The increased resolution also has implications for automated assignment and peak integration procedures. We selected a region of the ^{13}C-dispersed spectra of γGCS and used the automated peak picking procedure as implemented in nmrPipe (Delaglio et al. 1995). To ensure that the result reflects the increase in resolution and not the sensitivity of each spectrum, a weak cross-peak was used as an internal reference to define a threshold. 172 peaks were observed in the NOESY-PEP-HSQC while 287 could be picked and quantitatively analyzed in the HSQC-NOESY spectrum. Thus, the number of distance constraints was nearly doubled with the HSQC-NOESY.

Conclusion

The time-shared 3D HSQC-NOESY experiment presented here provides high resolution nOe cross-peaks with a simultaneous dispersion in the ^{13}C dimension for methyl protons and in the ^{15}N dimension for amide protons. This increase in resolution, at no cost in experimental time, is especially dramatic at the highest-field NMR spectrometers where more popular NOESY-HSQC-derived experiments would impart a much lower resolution in the dimension featuring nOes. Thus, when relaxation losses

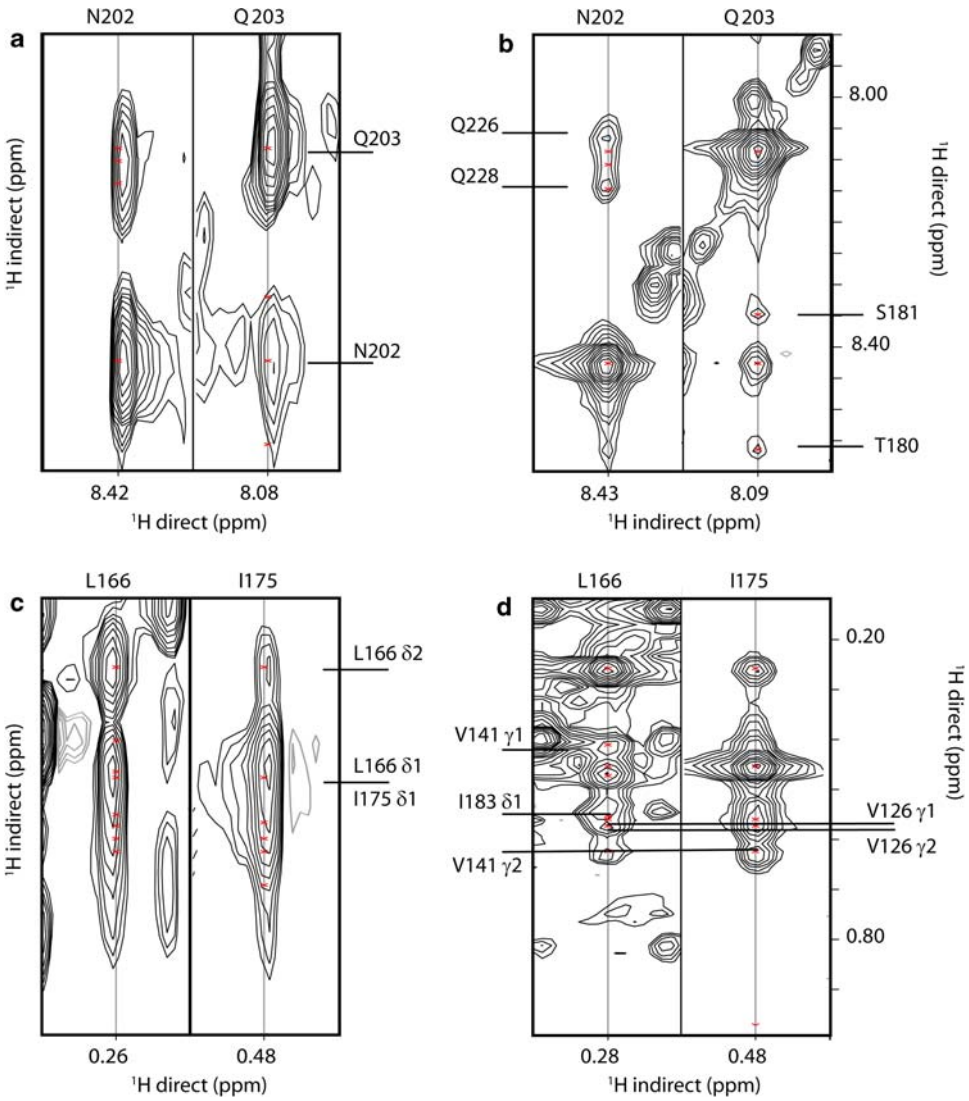

Fig. 3 Comparison of H/H 2D strips from the TS-NOESY-PEP-HSQC/TROSY experiment (**a** and **c**) or the TS-HSQC-NOESY experiment (**b** and **d**), obtained within the same amount of time for γGCS. **a**, **b** ^{15}N-dispersed spectra. **c**, **d** ^{13}C-dispersed spectra. Note that direct and indirect proton dimensions are swapped for **a** and **b** and for **c** and **d**

and the resulting sensitivity reduction is not an issue, it is preferable to use the TS-HSQC-NOESY rather than the TS-NOESY-HSQC family of experiments (Pascal et al. 1994; Uhrín et al. 2000; Xia and Zhu 2001; Frueh et al. 2006; Wurtz et al. 2007; Guo and Tugarinov 2009). This will be particularly valuable for α-helical proteins and unfolded proteins, in general, as well as for large proteins. The experiment is particularly suitable for ILV labelled proteins since all signals are distinct from the water resonance, which can hence be suppressed without affecting detection of nOe cross-peaks. For such samples, the optimal resolution then allows one to rescue the poor dispersion of methyl protons. Further improvements may be obtained in the indirect dimensions by using non-uniform sampling (NUS) (Schmieder et al. 1993; Rovnyak et al. 2004; Tugarinov et al. 2005; Hyberts et al. 2007, 2009) to optimize the resolution without dramatic increase in measurement time. Since long evolution times are then recorded in the indirect dimensions, TROSY variation, as suggested in the discussion above, should be beneficial, in particular for large proteins. Even without NUS, the use of the TS-HSQC-NOESY allows one to readily exploit the advantages of high-field instruments. This results in a dramatically increased number and improved quantification of distance constraints. This experiment was key in the successful determination of the structures of two large proteins of 37 kDa and 31 kDa. The experiment described here has helped to resolve many ambiguities in the crowded NMR spectra of these systems. The pulse sequences, together with an nmrPipe script to process the data, can be downloaded from http://gwagner.med.harvard.edu.

Acknowledgments This research was supported by the National Institutes of Health (grants GM 47467, CA127990 and RR 00995) and a Human Frontier Science Fellowship to A.K. A.K is currently a Director's fellow at the Los Alamos National Laboratory. We thank Dr. Ruma Banerjee for providing the construct for γGCS. We thank two anonymous reviewers for their comments on water suppression.

References

Barna JCJ, Laue ED, Mayger MR, Skilling J, Worrall SJP (1987) Exponential sampling, an alternative method for sampling in two-dimensional NMR experiments. J Magn Reson 73:69–77

Boelens R, Burgering M, Fogh RH, Kaptein R (1994) Time-saving methods for heteronuclear multidimensional NMR of (13C, 15N) doubly labeled proteins. J Biomol NMR 4:201–213

Brutscher B, Boisbouvier J, Pardi A, Marion D, Simorre J-P (1998) Improved sensitivity and resolution in 1H–13C NMR experiments of RNA. J Am Chem Soc 120:11845–11851

Chiarparin E, Pelupessy P, Ghose R, Bodenhausen G (1999) Relaxation of two-spin coherence due to cross-correlated fluctuations of dipole-dipole couplings and anisotropic shifts in NMR of 15N, 13C-labeled biomolecules. J Am Chem Soc 121:6876–6883

Delaglio F, Grzesiek S, Vuister GW, Zhu G, Pfeifer J, Bax A (1995) NMRPipe a multidimensional spectra processing system based on UNIX pipes. JBNMR 6:277–293

Farmer B II (1991) Simultaneous [13C, 15N]-HMQC, A pseudo-triple resonance experiment. J Magn Reson 93:635–641

Frueh DP, Arthanari H, Wagner G (2005) Unambiguous assignment of NMR protein backbone signals with a time-shared triple-resonance experiment. J Biomol NMR 33:187–196

Frueh DP, Vosburg DA, Walsh CT, Wagner G (2006) Determination of all nOes in 1H–13C-Me-ILV-U-2H–15N proteins with two time-shared experiments. J Biomol NMR 34:31–40

Frueh DP, Arthanari H, Koglin A, Vosburg DA, Bennett AE, Walsh CT, Wagner G (2008) Dynamic thiolation-thioesterase structure of a non-ribosomal peptide synthetase. Nature 454:903–906

Grzesiek S, Bax A (1993) The importance of not saturating H_2O in protein NMR. Application to sensitivity enhancement and NOE measurements. J Am Chem Soc 115:12593–12594

Guo C, Tugarinov V (2009) Identification of HN-methyl NOEs in large proteins using simultaneous amide-methyl TROSY-based detection. J Biomol NMR 43:21–30

Hyberts SG, Heffron GJ, Tarragona NG, Solanky K, Edmonds KA, Luithardt H, Fejzo J, Chorev M, Aktas H, Colson K, Falchuk KH, Halperin JA, Wagner G (2007) Ultrahigh-resolution (1)H-(13)C HSQC spectra of metabolite mixtures using nonlinear sampling and forward maximum entropy reconstruction. J Am Chem Soc 129:5108–5116

Hyberts S, Frueh D, Arthanari H, Wagner G (2009) FM reconstruction of non-uniformly sampled protein NMR data at higher dimensions and optimization by distillation. J Biomol NMR. doi: 10.1007/s10858-009-9368-1

Jerala R, Rule G (1995) A 3D 1H, 15N and 13C NOESY correlating experiment. J Magn Reson 108:294–298

Keller RLJ (2004) The computer aided resonance assignment tutorial. Cantina Verlag, Goldau

Koglin A, Mofid MR, Lohr F, Schafer B, Rogov VV, Blum MM, Mittag T, Marahiel MA, Bernhard F, Dotsch V (2006) Conformational switches modulate protein interactions in peptide antibiotic synthetases. Science 312:273–276

Kupce E, Muhandiram DR, Kay LE (2003) A combined HNCA/HNCO experiment for 15N labeled proteins with 13C at natural abundance. J Biomol NMR 27:175–179

Marion D, Ikura M, Tschudin R, Bax A (1989) Rapid recording of 2D NMR spectra without phase cycling. Application to the study of hydrogen exchange in proteins. JMR 85:393–399

Meissner A, Sorensen OW (1999) Suppression of diagonal peaks in TROSY-type 1H NMR NOESY spectra of 15N-labeled proteins. J Magn Reson 140:499–503

Orekhov VY, Ibraghimov IV, Billeter M (2001) MUNIN: a new approach to multi-dimensional NMR spectra interpretation. J Biomol NMR 20:49–60

Pascal S, Muhandiram D, Yamazaki T, Forman-Kay J, Kay L (1994) Simultaneous acquisition of 15N and 13C-edited NOE spectra of proteins dissolved in H_2O. J Magn Reson B 103:197–201

Perez-Trujillo M, Nolis P, Bermel W, Parella T (2007) Optimizing sensitivity and resolution in time-shared NMR experiments. Magn Reson Chem 45:325–329

Piotto M, Saudek V, Sklenar V (1992) Gradient-tailored excitation for single-quantum NMR spectroscopy of aqueous solutions. J Biomol NMR 2:661–665

Rovnyak D, Frueh DP, Sastry M, Sun ZY, Stern AS, Hoch JC, Wagner G (2004) Accelerated acquisition of high resolution triple-resonance spectra using non-uniform sampling and maximum entropy reconstruction. J Magn Reson 170:15–21

Sattler M, Maurer M, Schleucher J, Griesinger C (1995) A simultaneous 15N.1H and 13C, 1H-HSQC with sensitivity enhancement and a heteronuclear gradient echo. J Biomol NMR 5:97–102

Schmieder P, Stern AS, Wagner G, Hoch JC (1993) Application of nonlinear sampling schemes to COSY-type spectra. J Biomol NMR 3:569–576

Shaka AJ, Barker P, Freeman R (1985) Computer-optimized decoupling scheme for wideband applications and low-level operation. J Magn Reson 64:547–552

Shaka AJ, Keeler J, Frenkiel T, Freeman R (1983) An improved sequence for broadband decoupling: WALTZ-16. J Magn Reson 52:335–338

Sørensen O (1990) Aspects and prospects of multidimensional time-domain spectroscopy. J Magn Reson 89:210–216 1969

Talluri S, Wagner G (1996) An optimized 3D NOESY-HSQC. J Magn Reson B 112:200–205

Tugarinov V, Kay LE, Ibraghimov I, Orekhov VY (2005) High-resolution four-dimensional 1H–13C NOE spectroscopy using methyl-TROSY, sparse data acquisition, and multidimensional decomposition. J Am Chem Soc 127:2767–2775

Uhrín D, Bramham J, Winder SJ, Barlow PN (2000) Simultaneous CT-13C and VT-15N chemical shift labelling: application to 3D NOESY-CH3NH and 3D 13C, 15N HSQC-NOESY-CH3NH. J Biomol NMR 18:253–259

Wurtz P, Aitio O, Hellman M, Permi P (2007) Simultaneous detection of amide and methyl correlations using a time shared NMR experiment: application to binding epitope mapping. J Biomol NMR 39:97–105

Xia Y, Zhu G (2001) 3D Haro-NOESY-CH3NH and Caro-NOESY-CH3NH experiments for double labeled proteins. J Biomol NMR 19:355–360

Zhu G, Xia Y, Sze KH, Yan X (1999) 2D and 3D TROSY-enhanced NOESY of 15N labeled proteins. J Biomol NMR 14:377–381